

Transdermal photopolymerization for minimally invasive implantation

J. ELISSEEFF*, K. ANSETH†, D. SIMS‡, W. MCINTOSH*, M. RANDOLPH‡, AND R. LANGER*§

*Harvard-Massachusetts Institute of Technology Division of Health Sciences and Technology and Massachusetts Institute of Technology Department of Chemical Engineering, Cambridge, MA 02139; †Department of Chemical Engineering, University of Colorado, Boulder, CO 80309; and ‡Department of Surgery, Massachusetts General Hospital, Boston, MA 02114

Contributed by R. Langer, December 16, 1998

ABSTRACT Photopolymerizations are widely used in medicine to create polymer networks for use in applications such as bone restorations and coatings for artificial implants. These photopolymerizations occur by directly exposing materials to light in “open” environments such as the oral cavity or during invasive procedures such as surgery. We hypothesized that light, which penetrates tissue including skin, could cause a photopolymerization indirectly. Liquid materials then could be injected s.c. and solidified by exposing the exterior surface of the skin to light. To test this hypothesis, the penetration of UVA and visible light through skin was studied. Modeling predicted the feasibility of transdermal polymerization with only 2 min of light exposure required to photopolymerize an implant underneath human skin. To establish the validity of these modeling studies, transdermal photopolymerization first was applied to tissue engineering by using “injectable” cartilage as a model system. Polymer/chondrocyte constructs were injected s.c. and transdermally photopolymerized. Implants harvested at 2, 4, and 7 weeks demonstrated collagen and proteoglycan production and histology with tissue structure comparable to native neocartilage. To further examine this phenomenon and test the applicability of transdermal photopolymerization for drug release devices, albumin, a model protein, was released for 1 week from photopolymerized hydrogels. With further study, transdermal photopolymerization potentially could be used to create a variety of new, minimally invasive surgical procedures in applications ranging from plastic and orthopedic surgery to tissue engineering and drug delivery.

Fabricating polymers *in situ* provides many advantages for a variety of biomedical applications. For example, prepolymerized liquid solutions or moldable putties can be easily placed in complex shapes (e.g., tooth caries) and subsequently reacted to form a polymer of exactly the required dimensions. Little, if any, additional shaping or modification of the implant is required. The adhesion of the polymer to surrounding tissue is generally significantly improved because of intimate contact of the polymer with the tissue during formation and the mechanical interlocking that can result from surface microroughness. In addition to these advantages, however, *in situ* polymerization also introduces many new challenges. Polymerization conditions for *in vivo* applications are quite adverse, including a narrow range of physiologically acceptable temperatures, requirement for nontoxic monomers and/or solvents, moist and oxygen-rich environments, and the need for rapid processing and clinically suitable rates of polymerization. However, photopolymerizations can overcome many of these limitations because the initiation does not require elevated temperatures, and the polymerization process is typically rapid (a

few seconds to a couple of minutes), which allows the system to overcome oxygen inhibition and moisture effects.

The concept of using light to polymerize or cure materials *in vivo* has been practiced in accessible places such as the oral cavity in dentistry, during invasive surgery, and more recently through minimally invasive surgery, leading to potentially new methods to prevent restenosis after angioplasty and postsurgical adhesions (1–4). The above approaches require directly shining light on polymers to cause a photopolymerization, either as an open or invasive procedure. We hypothesized that enough light might traverse tissue, including skin, to cause a photopolymerization transdermally, and therefore provide a new method to implant biomaterials. Liquid biomaterials could be delivered s.c. through a small diameter needle and would be converted from a liquid to a solid after only minutes of skin exposure to light (Fig. 1A). Transdermal photopolymerization could effectively allow implantation of biomaterials for plastic surgery applications, including both biodegradable and nondegrading polymers, and potentially would enable cells or drugs to be injected and encapsulated for tissue engineering, drug delivery, or other applications. To test the concept of transdermal polymerization, a model polymer hydrogel system using poly(ethylene oxide) (PEO) was chosen (5). Hydrogels are candidate materials for many biomedical applications, including tissue engineering and drug delivery, because of their high water content, transport properties, and tissue-like physical and mechanical behavior (5).

METHODS

Light Penetration. Skin was shaven and harvested from all regions of a swine (Yorkshire, 6 months, Massachusetts General Hospital). Fifteen samples of swine skin were excised, and hair and fat were removed. Eleven human cadaver skin samples (Caucasian, National Institute of Disease Research, Bethesda, MD) ranging in thickness from 1.35 to 2.55 mm were cut into approximately 1-cm squares, and the s.c. fat was removed. Tissue thickness was measured by using a micrometer. Tissue hydration was maintained by a saline bath. An integrating sphere was connected to two monochromators with a 75-W lamp (Spex Industries, Edison, NJ) as described (6). Synchronous scans were performed from 250 to 550 nm with 2-nm increments, 0.1-s integration time, 1-mm slits, and 0-nm offset. Percent transmission was determined by dividing the detected transmitted light with tissue by the lamp synchronous scan without tissue present (background).

Transdermal Photopolymerization Kinetics. Differential scanning calorimetry (DSC, Perkin–Elmer, DSC7 with a photocalorimetric accessory) was used to monitor the polymerization rate of PEO dimethacrylates (PEODM) to determine

The publication costs of this article were defrayed in part by page charge payment. This article must therefore be hereby marked “advertisement” in accordance with 18 U.S.C. §1734 solely to indicate this fact.

PNAS is available online at www.pnas.org.

Abbreviations: PEO, poly(ethylene oxide); PEODM, PEO dimethacrylate; HPK, 1-hydroxycyclohexyl phenyl ketone; GAG, glycosaminoglycan.

§To whom reprint requests should be addressed at: 400 Main Street, E25-342, Cambridge, MA 02139. e-mail: rlanger@mit.edu.

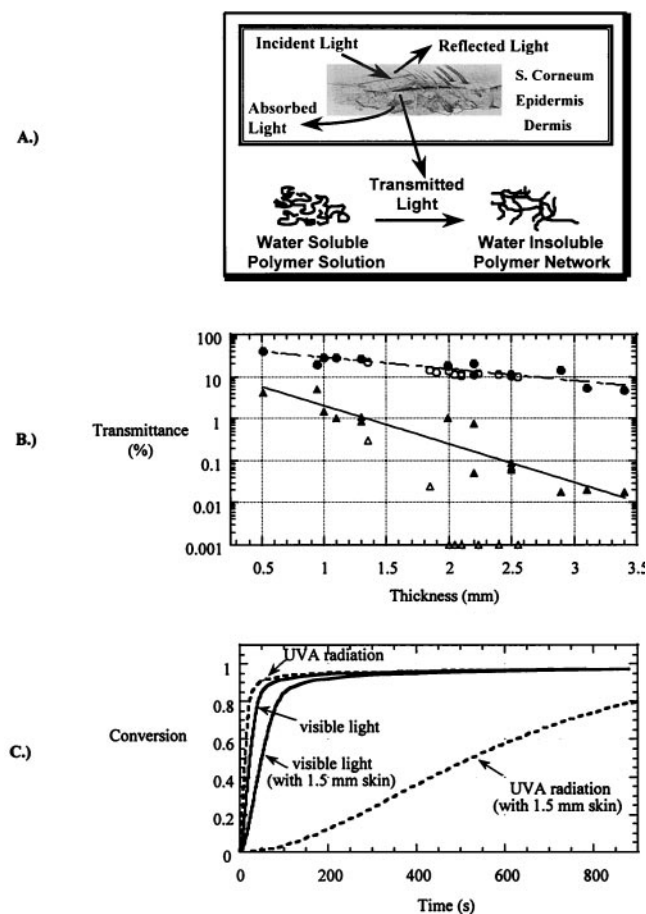


FIG. 1. (A) Schematic of transdermal photopolymerization. (B) Penetration of light through swine skin at 360 nm (\blacktriangle) and 550 nm (\bullet) and human skin at 360 nm (\triangle) and 550 nm (\circ). (C) Kinetics of transdermal photopolymerization of PEODM with UVA (dashed line), visible light (solid line) and beneath 1.5 mm human skin by using UVA (dashed line) and visible light (solid line) with an incident light intensity of 100 mW/cm² and 0.04% (wt/wt) photoinitiator.

kinetic constants. The photocalorimetric accessory included a monochromator to select light of a given wavelength, as well as neutral density filters to control the incident light intensity. Polymerizations were monitored at 37°C in the presence of oxygen. In a typical experiment, 5–10 mg of the PEODM (M_r 3,400, Shearwater Polymers, Huntsville, AL, 20% wt/vol in water) was placed in a DSC pan. A shutter was opened to expose the samples to light of the selected intensity and wavelength, and the polymerization rate was obtained. A kinetic model developed and described elsewhere was used to predict the polymerization rates and double bond (functional group) conversion during the photopolymerization (7). The model parameters were fit from the DSC rate data of PEODM by using the method of Anseth *et al.* (8). Parameters used for both the UVA and visible light simulation were as follows: kinetic constant for propagation, 105 liter/mol-s; monomer specific volume, 0.93 cc/g; polymer specific volume, 0.86 cc/g; thermal expansion coefficient of monomer, 0.0005/°C, of polymer, 0.000075/°C; T_g monomer, -100°C; T_g polymer, 0°C; concentration of initiator, 0.0025 M, monomer, 1 M. Visible light simulations used a calculated intensity of 20.69 mW/cm² (incident 100 mW/cm²), initiator efficiency of 0.50, and fractional change in volume of 50 cc/g. UVA simulations used a calculated light intensity of 0.045 mW/cm² (incident 100 mW/cm²), an initiator efficiency of 0.65, and a fractional change in volume of 150 cc/g.

Cellular Biocompatibility. Chondrocytes were plated at a density of 1×10^4 cells/cc in 12-well tissue culture plates.

Control wells consisted of no initiator or light and initiator only. 1-Hydroxycyclohexyl phenyl ketone (HPK) was added at desired concentrations from a stock solution (120 mg/ml). The plate was exposed to 1.5 mW/cm² UVA light for 2 min. After 24 hr, media were removed, and 1 ml MTT (1 mg/ml [3-(4,5-dimethylthiazol-2-yl)-2,5-diphenyl-2H-tetrazolium bromide]) was added and incubated for 1–3 hr. One milliliter of 0.04 N HCl in isopropanol was added to the wells and mixed on a rotating shaker for 30 min. Absorbance was read at 560 nm ($n = 3$).

Chondrocyte Encapsulation. Primary bovine chondrocytes were isolated as described (9). PEODM and PEO (M_r 100,000) were dissolved in PBS in a 2:3 ratio to make a 20% (wt/vol) solution. The photoinitiator HPK (Polysciences) was added to make a final concentration of 0.04% (wt/wt). Thirteen athymic female mice (6 weeks old, Charles River Breeding Laboratories) were anesthetized with methoxyfluorane and injected with four 0.1-ml aliquots of the polymer/cell suspension (50 million cells/cc) each. The mice were placed under a lamp (GloMark Systems, Upper Saddle River, NJ) emitting UVA radiation at an intensity of 2 mW/cm² for 3 min. The polymer/chondrocyte hydrogel was palpated to observe polymerization progression. Mice were sacrificed at 3 days and 2, 4 and 7 weeks by pentobarbital overdose. Total collagen and glycosaminoglycan (GAG) were determined by the hydroxyproline and dimethyl-methylene blue dye methods, respectively (10). Histology was performed according to standard procedure.

Albumin Release. BSA (Sigma) was added to the 50/50% (wt/vol) macromer solution of M_r 1,000, vortexed, and photopolymerized 1 min in scintillation vials to which 3 ml of PBS was added. A 5% (wt/wt) loading dose of albumin was encapsulated in the hydrogels. The gels ($n = 4$) were incubated at 37°C under sink conditions. At various time points the PBS was removed and frozen while 3 ml of fresh PBS was added. Albumin concentration was determined by using a micro BCA assay (Pierce).

RESULTS AND DISCUSSION

The first feasibility issue for transdermal photopolymerization involved the ability of light to penetrate skin. Human skin ranges in thickness from 0.5 mm over the tympanic membrane and eyelids to 6 mm on the back and soles of feet and hands, with an average thickness of 1–2 mm (11). Although light transmittance has been examined in the stratum corneum and epidermis, few studies have focused on full thickness skin, including the dermis (6, 12). The epidermis, typically only a fraction of 1 mm, contains chromophores that absorb radiation and impede the penetration of light. The dermis, ranging in thickness throughout the body, is responsible for the majority of light attenuation in full thickness skin (6, 12). Swine skin often is used as a model for human skin because of structural, functional, and biochemical similarities (13–15). The transmittance of light through swine and human skin was analyzed from 250 to 550 nm. Fig. 1B demonstrates the transmittance of skin at 360 and 550 nm, wavelengths in the UVA and visible light ranges, respectively, where common photoinitiators have maximal efficiency. All skin samples exhibited decreasing light transmittance as tissue thickness increased. Longer wavelengths of light were able to penetrate deeper through the tissue, while the transmittance of human skin in the UVA region was markedly reduced compared with swine skin, with no UVA light penetrating human skin greater than 2 mm in thickness. Human and swine skin demonstrated similar absorption in the visible light region analyzed (400–550 nm, Fig. 1B). Thus, swine skin provides an appropriate model for light transmittance through human skin only in the visible light range. Transdermal photopolymerization through human skin will be most efficient by using visible light and the corresponding visible light photoinitiators.

The time required to transdermally photopolymerize a hydrogel under skin was examined by using a kinetic model for photopolymerizations and the experimental percent transmittance of light determined in Fig. 1B (see *Methods*). Fig. 1C portrays the conversion versus time of PEODM (M_r 3,400) under 1.5-mm human skin using visible or UVA light and without skin present. An incident light intensity of 100 mW/cm² (used clinically in phototherapy) and 0.04% (wt/wt) photoinitiator were used for the simulations (16). UVA photoinitiators have a higher efficiency than visible light photoinitiators, yet the penetration of visible light through human skin is greatly enhanced compared with UVA radiation (see parameters for simulation in *Methods* and Fig. 1B) (17). The primary influence of light attenuation in tissue is a decrease in polymerization rate and an increase in polymerization time. While the conversion of PEODM beneath human skin by using visible and UVA radiation does not largely differ after 15 min (900 s), the visible light polymerization reaches over 80% conversion (and has formed a mechanically stable network) after only 100 s of skin exposure to light. Even under skin with minimal light transmittance, polymerization times required for transdermal photopolymerization under skin are short, clinically feasible times, on the order of minutes (Fig. 1C).

To examine the cellular toxicity of transdermal photopolymerization, we studied the effects of the activated photoinitiator on chondrocyte (a model cell for tissue engineering) metabolism. The worst case scenario of all radicals available to damage cells was examined by excluding the polymer, which reacts with the radical species formed by photoinitiator exposure to light. Fig. 2 demonstrates the effect of increasing photoinitiator concentration (HPK) in complete media on cell metabolism as determined by 3-(4,5-dimethylthiazol-2-yl)-2,5-diphenyl-2H-tetrazolium bromide (MTT) activity located in the mitochondria and cytoplasm. A decrease in chondrocyte MTT activity with increasing HPK concentration is observed after exposure of the cells and initiator to light compared with controls (Fig. 2A). Low photoinitiator concentrations (0.01–0.04% wt/vol) caused no detectable chondrocyte damage, yet still allowed photopolymerization to occur as demonstrated in the polymerization kinetics in Fig. 1C. These initiation conditions subsequently were used for optimal cell encapsulation during photopolymerization.

One envisioned application for transdermal photopolymerization and simultaneous photoencapsulation of cells is tissue engineering. A minimally invasive technique to tissue engineer cartilage would provide many benefits in plastic surgery. For example, cell and macromer solutions could be injected underneath the skin, molded to the desired shape, and subsequently photopolymerized, circumventing the need for any surgical incisions. The cartilage formed from the *in situ* molded and polymerized gel would be beneficial for augmentation

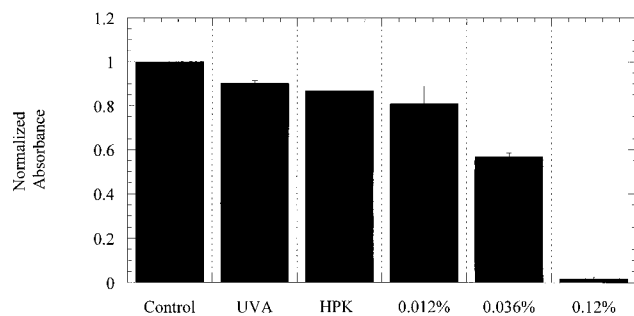
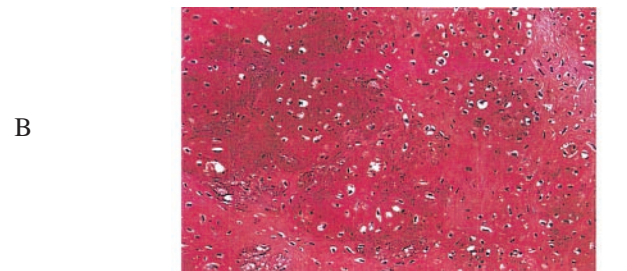
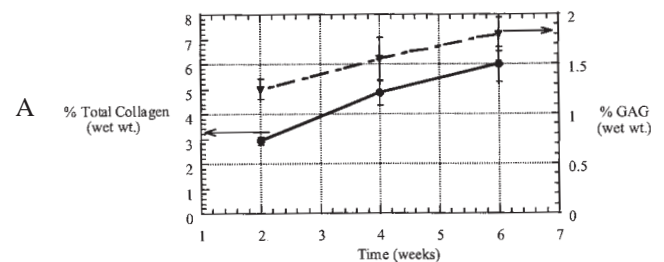
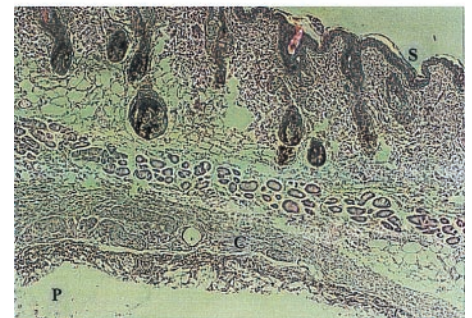


FIG. 2. Normalized 3-(4,5-dimethylthiazol-2-yl)-2,5-diphenyl-2H-tetrazolium bromide absorbances of chondrocytes after exposure to 1.5 mW/cm² UVA light and HPK (% wt/vol). Control cells were not exposed to initiator or light, HPK control (0.036% HPK) was not exposed to light, and UVA control cells were exposed to light only.

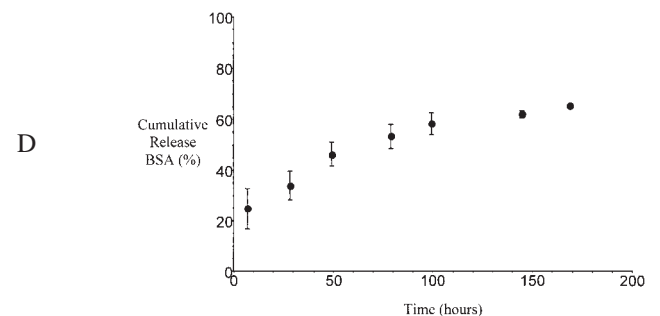
reconstructive surgeries. The encapsulation and implantation of bovine chondrocytes in athymic mice was used to further assess the cellular compatibility of transdermal photopolymerization. Cartilage is comprised of chondrocytes surrounded by an extracellular matrix of collagen and proteoglycans. Chondrocytes were encapsulated subcutaneously in a PEO semi-interpenetrating network (semiIPN) via transdermal photopolymerization. The semiIPN system provides a porous hydrogel where PEO not covalently crosslinked can diffuse from the implant, providing potential space for chondrocyte growth and matrix production. The photopolymerized constructs were harvested after 2, 4, and 7 weeks, and total collagen and GAG contents were determined (Fig. 3A). Both the GAG and total collagen contents increased with time, demonstrating the formation of neocartilage with extracellular matrix contents



B



C



D

FIG. 3. (A) Total collagen and GAG contents (per construct wet weight) of chondrocytes encapsulated and implanted by transdermal photopolymerization. (B) Safranin O-stained histological section of neocartilage 6 weeks postimplantation ($\times 200$). (C) Hematoxylin/eosin-stained section of an implanted hydrogel (P, without cells), surrounded by a fibrous capsule (C), s.c. tissue and skin (S). (D) Release of BSA from PEODM (M_r 1,000) hydrogels over 200 hr.

comparable to other tissue engineering systems using poly(glycolic acid), and PEO scaffolds (9, 18). Fig. 3B is a Safranin O-stained histology section of tissue formed after 6 weeks implantation in athymic mice via transdermal photopolymerization. Safranin O stains negatively charged proteoglycans (GAGs) secreted by differentiated chondrocytes, which is distributed throughout the tissue section. The chondrocytes are viable, and necrosis is not observed. The histology exhibits structures typical of neocartilage, including ovoid cells in lacunae surrounded by an extracellular matrix rich in GAG. These results confirm that the cells not only survived implantation by transdermal photopolymerization but also produced tissue resembling neocartilage. These preliminary results demonstrate the potential use of transdermal photopolymerization for cartilage tissue engineering applications. Furthermore, hydrogels without chondrocytes were implanted via transdermal photopolymerization to observe the tissue response to implantation and the semiIPN. Fig. 3C shows the skin, s.c. tissue, and hydrogel in a mouse 3 days after implantation. No light damage, characterized by pyknotic nuclei, is observed in the skin. The implanted polymer is surrounded by a fibrous capsule with inflammatory cells (polymorphonuclear leukocytes, lymphocytes, and giant cells), demonstrating a foreign body response comparable to other biomaterials such as prostaglandin (19). These experiments suggest biocompatibility of the transdermal photopolymerization process and the hydrogel implant.

In addition to the potential applications in tissue engineering, transdermal photopolymerization may be applied to the implantation of polymers for drug delivery. Transdermal photopolymerization would allow physicians to implant polymer delivery devices without the need for surgical intervention, thus providing an inexpensive method with reduced risk to the patient and potentially newfound applications. In contrast to methods that inject microparticles, these monolithic devices would have minimal migration, maintain localized delivery, and could be easily removed if needed. As an illustration for this application, BSA (M_r 6,800) was photopolymerized in PEO hydrogels (M_r 1,000), and release was observed for the duration of the experiment (Fig. 3D).

Future studies should aim to identify more efficient, biocompatible photoinitiators, particularly in the visible wavelength regions, where light penetration through skin is greater, and new, photopolymerizing polymers. Furthermore, other

cell types could be encapsulated for tissue engineering or related purposes.

We are indebted to Dr. Nikiforos Kolias and Robert Gillies at the Wellman Laboratories of Photomedicine, Massachusetts General Hospital, for assistance with the skin penetration experiments. This work was supported by Advanced Tissue Sciences, La Jolla, CA and National Institutes of Health Grant 1-RO1DE13023-01, 1998.

- Hill-West, J., Chowdhury, S., Slepian, M. & Hubbell, J. (1994) *Proc. Natl. Acad. Sci. USA* **91**, 5967–5971.
- Hill-West, J., Dunn, R. & Hubbell, J. (1995) *J. Surg. Res.* **59**, 759–763.
- Sawhney, A., Lyman, F., Yao, F., Levine, M. & Jarrett, P. (1996) *Proc. Int. Symp. Controlled Release Bioact. Mater.* **23**, 236–237.
- Watts, D. C. (1992) in *Materials Science and Technology: A Comprehensive Treatment*, ed. Williams, D. F. (VCH, New York), Vol. 14, pp. 209–258.
- Peppas, N. (1987) *Hydrogels in Medicine and Pharmacy* (CRC, Boca Raton, FL), Vol. II.
- Anderson, R. R. & Parrish, J. A. (1982) in *The Science of Photomedicine*, eds. Regan, J. D. & Parrish, J. A. (Plenum, New York), pp. 147–194.
- Anseth, K. S. & Bowman, C. N. (1994) *Chem. Eng. Sci.* **49**, 2207–2217.
- Anseth, K., Wang, C. & Bowman, C. (1994) *Polymer* **35**, 3243.
- Freed, L. & Vunjak-Novakovic, G. (1995) in *The Biomedical Engineering Handbook*, ed. Bronzind, J. (CRC, Boca Raton, FL), pp. 1778–1796.
- Farndale, R., Buttle, D. & Barrett, A. (1986) *Biochim. Biophys. Acta* **883**, 173–177.
- Woodburne, R. T. & Burkell, W. E. (1994) *Essentials of Human Anatomy* (Oxford Univ. Press, New York).
- Bruls, W., Slaper, H., van der Leun, J. & Berrens, L. (1984) *Photochem. Photobiol.* **40**, 485–494.
- Walker, M., Hulme, T., Rippon, M., Walmsley, R., Gunnigle, S., Lewin, M. & Winsey, S. (1997) *J. Pharm. Sci.* **86**, 1379–1384.
- Meyer, W. (1996) *Hautarzt* **47**, 178–182.
- Fourtanier, A. & Berrebi, C. (1989) *Photochem. Photobiol.* **50**, 771–784.
- Parrish, J. A. (1982) in *The Science of Photomedicine*, eds. Regan, J. D. & Parrish, J. A. (Plenum, New York), pp. 3–18.
- Odian, G. (1991) *Principles of Polymerization* (Wiley, New York).
- Sims, D., Butler, P., Casanova, R., Lee, B., Randolph, M., Lee, W. P. A., Vacanti, C. & Yaremchuk, M. (1996) *Plast. Reconstr. Surg.* **98**, 843–850.
- Anderson, J. M. (1988) *Trans. Am. Soc. Artif. Intern. Organs* **XXXIV**, 561–571.